OXIDATIVE STRESS AND TRABECULAR MESHWORK CELLS IN BIOMIMETIC THREE-DIMENSIONAL ENVIRONMENTS: IMPLICATIONS FOR GLAUCOMA

by

Kathryn A. Scherrer

A thesis submitted to the Faculty and the Board of Trustees of the Colorado School of Mines in partial fulfillment of the requirements for the degree of Master of Science (Quantitative Biosciences and Engineering).

Golden, Colorado

Date_____

Signed: _____

Kathryn A. Scherrer

Signed: _____

Dr. Melissa D. Krebs
Thesis Advisor

Golden, Colorado

Date_____

Signed: _____

Dr. John R. Spear
Professor and Department Head
Department of Quantitative Biosciences and Engineering

ABSTRACT

Glaucoma is a term for a collective group of degenerative eye diseases which cause damage to the optic nerve, eventually causing a characteristic vision loss. The main risk factor for glaucoma is increased intraocular pressure, often caused by an imbalance of aqueous humor generation or impaired drainage through the trabecular meshwork (TM) outflow tissue. The disfunction or blockage of the TM is frequently linked to cell reactions or apoptosis from oxidative stress. The small size, delicate composition, donor tissue limitations, and high structural complexity of the trabecular meshwork make it difficult to research with good accuracy, as the relationship between cells and their extracellular environment has numerous variables. Thus, a biomaterial-based approach was considered more appropriate for providing a cell culture environment with greater mimicking abilities to the native TM. The 3D models fabricated allowed for studies of oxidation consequences of hydrogen peroxide and transforming growth factor β2, along with drug delivery *in vitro* to be more representative of the inner eye.

In this work, human TM (hTM) cells were cultured on two distinct 3-dimensional matrices to better understand how the cells respond to changes in their surrounding environment. Collagen scaffolds with four varying compositions of glycosaminoglycans were utilized for the known structural similarity to the native TM, while alginate-chitosan hydrogels were fabricated in order to incorporate a drug delivery system into the 3D model. Cellular response was measured by using assays including those of relative cell activity and reactive oxygen species, along with quantitative expression of several fibrotic extracellular proteins. It was found that the hTM cells had significantly different responses to stimuli when grown on the traditional 2D tissue culture plates in comparison to the novel 3D collagen scaffolds, showcasing a greater

resistance to cell death and altered levels of fibrotic mRNA and protein expression. Furthermore, the hydrogels were determined to be a viable 3D culture method for hTM cells, with their protein release abilities successfully modeled with myoglobin highlighting potential areas for oxidative agent or antioxidant exposure. Several novel therapeutics were studied for their antioxidant potential to contribute to this aspect, with the greatest promise found with CNPs and peptain-1. This work will help provide insights into the behavior of hTM cells when grown in a biomimetic manner more similar to their native 3D tissue when introducing stimuli to their surrounding microenvironment.

TABLE OF CONTENTS

LIST OF FIGURES

LIST OF TABLES

ACKNOWLEDGEMENTS

I would like to thank my advisor Dr. Melissa Krebs, who was a fantastic mentor always ready to help and offer calming advice. Working for her as an undergrad encouraged me to pursue a Master's degree in the first place. Thank you also to Dr. Matt Osmond, who first introduced me to the lab and showed me all the basics I used in my own research, and who would always know where to find even the most obscure lab supplies. I am grateful to Bikram and Michael for teaching me different techniques and parts of their own work to merge into mine, and for helping troubleshoot. And thank you to all the professors (especially guest speaker Dr. Mina Pantcheva who recruited me for glaucoma research in the first place) I had at Mines who were inspiring and supportive when it came to learning how to be an engineer. Also thank you to Dr. Nanette Boyle and Josh Ramey for taking their time to be on my committee.

Most importantly I want to thank my mother for her always being there, my father for reminding me to find time to have fun, and to all my other family and friends. I dedicate this to my mom and grandfather who was my number one supporter in going to college to better educate myself but who passed before he could see me finish. And finally, a special thank you to my cat Zwitter (and his sister Cami). He's the best listener and I may have never made it through getting my degrees without having him come running to greet me at the door while purring after a long day.

CHAPTER ONE: INTRODUCTION

1.1 Glaucoma Background

Glaucoma is a group of related eye diseases causing damage to the optic nerve, which can result in vision loss or blindness even with treatment.[1] It is currently the second leading cause of blindness in the world, following cataracts. However, while cataracts can be removed with corrective surgery and an artificial lens implant, glaucoma currently has no cure.[1,2] Known as the "silent thief of sight," glaucoma slowly damages the eyes and causes irreversible harm.[3] Approximately three millions Americans live with the disease with an estimated 80 million cases worldwide, where more than half of the affected people are unaware they have glaucoma as there are often no early symptoms.[1] In the United states alone, there have been over one hundred thousand people who have gone blind from this disease.[4] Even with treatment, glaucoma will cause approximately 15% of people affected by it to become blind in at least one eye within twenty years of onset.[5]

The encompassing term of glaucoma is used generically to cover several variations of damage to the optic nerve: primary and secondary open-angle glaucoma, angle-closure glaucoma, normal-tension glaucoma, pigmentary glaucoma, and glaucoma found in children often from anatomical problems. The exact cause of the disease remains unknown, although risk factors have been identified. Those over the age of sixty, of African, Asian or Hispanic descent, who have a family history of glaucoma, manage other medical conditions, thin corneas, have poor eyesight, eye injuries, or are taking corticosteroid medications are more likely to develop glaucoma.[5]

High internal eye pressure (intraocular pressure or IOP) is the most prevalent and concerning of risk factors to date. The eye contains a fluid known as the aqueous humor, which normally

drains through a tissue called the trabecular meshwork (TM) located at the iris cornea junction. This fluid is responsible for providing nutrients to the lens and cornea, acting as the equivalent of a blood supply to the front of the eye.[6] Impaired drainage or overproduction of aqueous humor results in abnormal buildup of the fluid and elevated IOP, going anywhere over the normal range of 12 to 22mmHg.[4,5] While there is a strong correlation between high internal eye pressure and incidence of glaucoma, it is not a guarantee. Some individuals with high eye pressures will never develop glaucoma, while others with glaucoma and IOP in the normal range exist as well.[4]

Primary open-angle glaucoma (POAG) is the most common form of the disease, accounting for around 70% of cases across the globe. In POAG, there is nothing abnormal about the rate of fluid production for the aqueous humor; rather, the drainage is either blocked by what is typically protein buildup, or the pores of the TM have narrowed.[7] This in turn increases the intraocular pressure and damages the optic nerve. The IOP is the only modifiable risk factor for those with glaucoma.[8]

1.2 Current Treatments

Symptoms which alert individuals to having glaucoma cover a wide range of possibilities, including patchy blind spots in peripheral or central vision, tunnel vision, or severe headaches. Eye pain, nausea, vomiting, blurred vision, halos around lights, and eye redness may be present in angle closure cases.[9] However, many forms of glaucoma have no warning signs until the condition has reached a highly progressed stage and damage has already occurred to the optic nerve. Open-angle glaucoma is the most common version, where the trabecular meshwork does not function properly so that IOP gradually increases. The onset is so slow that vision loss often occurs before the person is aware there is a problem due to symptom appearance.[5]

All forms of POAG rely on the same standard treatment mechanisms, although all of which are not cures but may prevent or prolong the onset of symptoms and damage. The two routes of action are to either slow the rate of aqueous humor production or to increase the rate of aqueous humor drainage through the trabecular meshwork and the uveoscleral pathway. The treatment comprises of laser treatment, incisional surgery, or medication. Medicinal means are the traditional first approach, especially simple monotherapies which have been found to increase compliance and decrease adverse reactions and side effects. The five standard drug classes in use are prostaglandin analogs, beta blockers, diuretics, cholinomimetics, and alpha agonists. The goal is to lower IOP by twenty-five percent or more once a patient has been placed onto one or several of these drugs, although a more dramatic decrease would be favorable for severe cases. Unfortunately, a thirty percent reduction is about the highest that can be achieved through medication, with many individuals not responding sufficiently. Invasive procedures with physical alteration of the eye structure through lasers or cutting are then relied upon, providing temporary relief.[8]

Future treatments are hoped to expand the mechanisms of action, and directly target the trabecular meshwork. Theories include ion channel blockers to decrease cell apoptosis and necrosis, various vitamins for improving cell health, increasing blood flow for drainage purposes, and introducing antioxidants to better the physical environment of the eye.[8] Ideally, the treatments would permanently alter the physical structure of the trabecular meshwork to offer a cure for the elevated IOP, thus mitigating what is considered one of the main risk factors for glaucoma.

1.3 Structure and *In Vitro* Models of the Trabecular Meshwork

The trabecular meshwork is a small porous tissue of triangular shape, composed of connective tissue beams and sheets covered with TM cells. The meshwork can be further broken down into the uveal meshwork, corneoscleral meshwork, and juxtacanalicular (JCT) region which are all responsible for filtering the aqueous humor. The tissue is organized of components such as collagen, laminin, elastin, fibronectin, and glycosaminoglycans (GAGs) among other proteins. Porous, intratrabecular spaces within the TM promote the passage of the aqueous humor out of the inner eye, through the inner wall of the Schlemm's canal, into the collector channels, and into the blood stream. The JCT region is thought to be the location of main resistance to outflow.[10]

Traditionally, TM cells have been studied with the use of two-dimensional cell culture dishes *in vitro*. Cells on tissue culture plates are the most common model to study cell biology and physiology.[11] This may be the typical and relatively simple method of study, but that does not make it the most accurate. The 2D cultures do not effectively mimic the effect of the complex microarchitecture structure and biological signals found in the natural TM. Signaling is one of the key components that turns a group of cells into a tissue and part of a larger organizational network, influencing cell proliferation, migration, adhesion, structure, and extracellular matrix (ECM) deposition.

Several functioning models of the TM in a 3D manner have been created previously. One of the first was TM cells cultured on microfabricated SU-8 porous structures, gelatin-coated SU-8 meshes. Due to the system only having a thickness of ~20μm, the cells are not able to migrate in a truly 3D manner, so that the cells are only exposed to topographical cues.[12] An expansion on this work has looked into using the SU-8 porous structures to culture Schlemm's canal cells, the

location into which the aqueous humor drains. It was found that coating the structures with a hydrogel containing hyaluronic acid (HA) greatly improved cell attachment and proliferation, demonstrating the importance GAGs play in modeling the TM.[13] TM cells have also been cultured using materials such as Matrigel and MAX8.[14–16] A more recent model is a hydrogel composed of collagen type I, elastin-like polypeptide, and HA with photoactive functional groups. It has proved a viable 3D environment for TM cells which respond with expected stiffening under simulated glaucoma conditions.[17]

In the Krebs lab, there has been significant work on expanding the functionality of 3D models for the TM. Collagen scaffolds mixed with GAGs such as HA and chondroitin sulfate (CS) have been fabricated in either an aligned or non-aligned manner with freeze casting to create a porous environment. TM cells have been found to be viable and proliferated up to 3 weeks after seeding, where the cells migrated down within the 0.3mm scaffold thickness, reflecting the topography and alignment of the scaffold structure in an closer imitation of the native TM.[18,19]

Additionally, polymerized hydrogels composed of alginate and chitosan have been thoroughly investigated as a method of sustained drug delivery over time, designed for use in growth plate injuries, but were here applied to the trabecular meshwork as well.[20] This composition of hydrogel is well studied in literature, where it has been found that the polymerized hybrid fibers promote favorable biological responses. Alginate provides functional groups for cell attachment and proliferation, particularly when bound to the RGD motif, and the stiffness of the chitosan provides structure for the scaffold.[21] When combined, the pair will form a polyelectrolyte complex (PEC) due to hydrostatic interactions.

1.4 Importance of Reactive Oxygen Species and TGFβ2

Reactive oxygen species (ROS) is a collective term which encompasses oxygen free radicals such as superoxide, hydroxyl, peroxyl, and hydroperoxyl, in addition to nonradical oxidizing agents which can be easily converted to a free radical state; these include hydrogen peroxide, hypochlorous acid, and ozone. ROS are naturally involved in many biochemical processes, including metabolism, enzymatic reactions, electron transport in the mitochondria, and gene expression among others. Due to the nature of ROS molecules, they contain at least one unpaired electron, making them highly reactive and unstable substances which may easily cause damage or mutations to living cells. The body has natural defenses which break down ROS such as superoxide dismutase, catalase, glutathione peroxidase, vitamin E, and others.[22] When the balance shifts and ROS become more dominant, an oxidative stress environment is created which has been linked to many diseases: cancer, asthma, pulmonary hypertension, and retinopathy.[23]

Oxidative stress can be induced into cell culture environments with the use of chemical reagents. Hydrogen peroxide is the one of the most easily available and inexpensive options to provoke such a change. On its own it is a poorly reactive ROS, but it is able to easily pass through the cell membrane unlike full reactive oxidative molecules which have a charge that inhibits them. When added in sufficient amount, hydrogen peroxide may escape being converted by cell defenses into water and may instead become a free radical due to its naturally unstable nature.[22] A more indirect route of triggering oxidative stress is through the use of the cytokine transforming growth factor. This protein is present in several subtypes, including the alpha version, and beta isoforms 1, 2 and 3. It is the most potent pro-fibrotic cytokine and has been found in increased expression in nearly every fibrotic disease. When out of balance in its active form, TGFβ2 has been found to increase mitochondria ROS production and decrease

antioxidants naturally present in the body. Additionally, it upregulates the NOX genes which produce NADPH oxidases responsible for catalyzing the production of superoxide from NADPH and oxygen.[24,25] Anywhere from 1 to 2ng/mL is considered a normal level of TGFβ2, with POAG levels averaging 4ng/mL but ranging to nearly 10ng/mL.[26]

Oxidative stress is known to play a role in POAG, although the mechanisms of how the increase in ROS initially occur are not well understood. Oxidative stress can trigger damage to mitochondria, inflammation, endothelial dysregulation and dysfunction, and hypoxia. All of these aspects will eventually trigger apoptosis, contributing to glaucoma-related cell death. The cells that survive are not left unscathed, as it has been found that the proteomic reading of the aqueous humor is significantly altered in POAG as a direct results of TM damage from oxidation.[27] Note that oxidative stress does not trigger overnight and will instead take anywhere from weeks to years to develop.

1.5 Antioxidants for Glaucoma

As oxidative stress is a known factor leading to trabecular cell malfunction and apoptosis in glaucoma, finding a suitable antioxidant is a highly prioritized research area. The deficiency of several vitamins naturally occurring in human diets have been linked as variables in causing or aggravating existing glaucoma. Retinal ganglion cells have been found to experience significantly increased cell death when Vitamin E is deficient under glaucoma conditions.[28] The increased cell death is thought to be associated with increased levels of lipid peroxidation, which have in turn been found to be linked to Vitamin A deficiencies. Increased levels of Vitamin A have been considered as a potential antioxidant in the fact that it is able to reduce lipid peroxidation in a dose-dependent manner.[28,29] Other naturally occurring substances to influence the health of the eye include Vitamin C, Coenzyme Q, lipoic acid, and omega fatty acids to name

a few. Numerous antioxidants have also been subjected to clinical trials with the goal being to improve the oxidative environment of those with glaucoma. It has been found that combining several antioxidants at a single time can help to improve overall results, but this leads to difficulties with patient compliance.[30]

Two novel substances were identified for their potential use as an antioxidant to fight oxidative environments in glaucoma. The first is a molecule termed peptain-1, which was originally discovered in 2006 as a 21 amino acid core peptide found within the alpha-crystallin domain of αB-crystallin. It was noted that this segment (DRFSVNLDVKHFSPEELKVKV) had the ability to function as a molecular chaperone like its parent protein, preventing the aggregation and precipitation of proteins.[31] Research has since shown that peptain-1 is able to block lens epithelial cell apoptosis and cataract formation in rat pups and reduce stress-induced apoptosis in cell cultures.[32,33] Most recently, peptain-1 treatment was found to inhibit retinal ganglion cell death and axonal loss in rats with elevated IOP.[34] Due to its promise as a neuroprotection agent in glaucoma, it was decided to also investigate its ability to function as an antioxidant in the trabecular meshwork.

The second novel drug is termed cerium oxide nanoparticles (CNPs), which have gained attention in the last decade for regenerative antioxidant potential. CNPs have traditionally industrial applications, used in catalysts, polishers, and toxic gas removal.[35] However, it has been discovered they possess the ability to scavenge reactive oxygen and nitrogen species, making them effective against pathologies related to chronic oxidation and inflammation. Toleration for the nanoparticles *in vivo* has led to their identification as a potential agent for nanobiology studies and regenerative medicine.[35,36] Thanks to the promise of a therapeutic, CNPs were one of the antioxidants studied in this research.

Additionally, an accepted antioxidant was explored as a type of control for the peptain and CNP studies. Resveratrol (RSV) is a naturally occurring polyphenol found in plant species, particularly grapes, which has shown great promise as an antioxidant.[37] Previous work has shown RSV decreases intracellular ROS and inflammatory markers in trabecular meshwork cells, making it a suitable anti-oxidative and anti-apoptotic agent, although it was not shown to impact proteomic expression.[38] Due to its record of serving as a plausible antioxidant for the TM, it was the third and final antioxidant used in these studies.

1.6 Research Rationale

The purpose of the research conducted was to demonstrate the vitality of having a functional 3D model to more accurately depict the trabecular meshwork and how it can be used to better study and understand the impact of these cells to biological signals and oxidative stress. The response of hTM cells when they are able to grow in their native 3D structure can be vastly different than those grown in the traditional 2D cell culture technique. 3D culture systems are relatively lacking due to their complexity, although their importance is unquestionable as it has been found that trabecular meshwork cells have different functions and morphologies when placed in distinct topographical envionments.[39]

Here, two separate 3D environments were investigated to attempt a better understanding of the TM tissue. Collagen scaffolds combined with GAGs to more closely mimic the native composition of the TM were fabricated to provide a porous matrix for the cells to grow on. This culture method enabled a more realistic representation of the trabecular meshwork for *in vitro* studies while investigating hTM cell response to drugs and oxidation.

Additionally, alginate-chitosan hydrogels were crafted to attempt to mimic the progression of oxidative stress environments which develops in many patients. In cell culture studies, drugs

such as hydrogen peroxide and TGF are added either at a single point or every few days at a constant concentration. In reality, the oxidative environment develops slowly over time, making this an oversimplified method. Alginate-chitosan gels are a well recorded method of making polyelectrolyte complexes held together by electrostatic binding strengthened by the addition of cations such as calcium.[20] These are known to serve as scaffolds promoting cell growth as well as a drug delivery system.[40] The intention of using them in this research was to not only create a 3D environment for the growth of the cells as a way to model the native trabecular meshwork, but to also see how their bioresponse is altered with slow exposure to agents inducing oxidative stress.

CHAPTER TWO: MATERIALS AND METHODS

2.1 Materials

To fabricate the collagen scaffolds, fibrillar collagen type I was obtained from Collagen Matrix (Oakland, NJ), with the GAGs of chondroitin sulfate from shark cartilage, and hyaluronic acid sodium salt from *Streptococcus equi* from Sigma-Aldrich (St. Louis, MO). Glacial acetic acid was procured from Thermo Fisher Scientific (Waltham, MA) and phosphate buffer solution (PBS) from Invitrogen (Carlsbad, CA).

For the creation of the hydrogels, products included calcium sulfate dihydrate and low molecular weight chitosan from Sigma-Aldrich. Protanal LF 20/40 alginate was a generous gift from FMC BioPolymer (Philadelphia, PA). Myoglobin derived from equine skeletal muscle was purchased from Fisher Scientific.

All cells used were human trabecular meshwork cells purchased from ScienCell Research Laboratories (Carlsbad, CA) or Cell Applications (San Diego, CA), confirmed to be of hTM cell type after an increase in the expression of myocilin was observed after treatment with dexamethasone from Signma.[41] Low glucose Dulbecco's Minimum Essential Media (DMEM-LG) and streptavidin-CY3 were purchased from Invitrogen. The anti-elastin antibody was obtained from Abcam (Cambridge, UK) and goat anti-rabbit IgG from Dako (Denmark). High-Capacity cDNA Reverse Transcription kit and PowerUp SYBR Green master mix were gathered from Applied Biosystems (Foster City, CA). TGFβ2 was purchased from Sigma-Aldric, along with the BCA protein assay kit, 30% hydrogen peroxide stock, Triton X-100, H2DCFDA, and penicillin streptomycin. Fetal bovine serum (FBS) and goat serum originated from Fisher Scientific. The cell counting kit 8 (CCK-8) was obtained from Dojindo Molecular Technologies

(Rockville, MD). For the antioxidants, resveratrol was from Sigma-Aldrich, peptain-1 a gift from the lab of Professor Nagaraj at CU Anschutz, and the CNPs a gift from Professor Seal at the University of Central Florida.

2.2 Fabrication of Collagen Scaffolds

Collagen scaffolds were fabricated with the methods previously determined in the Krebs lab. Four different compositions were chosen to best mimic the native TM, which is primarily made out of collagen and GAGs.[10] Mixtures of collagen-only (CO), collagen-CS, collagen-HA, and collagen-CSHA were manufactured. This began by making a collagen slurry with 150mg of Collagen Type 1 mixed in 20mL of 0.05M acetic acid, and 10mL of the corresponding GAG. For the plain collagen scaffold, an additional 10mL of acetic acid were added. The final compositions of the others were 0.15wt% CS and HA, and 0.075wt% CSHA respectively. This resulted in a final mixture of 0.5wt% collagen and 0.05wt% total GAG.[18]

After the slurry was allowed to refrigerate overnight at 4ºC, 605µL of a slurry was added to a single well in a 24-well plate. The 1.5cm diameter of the well in combination with the volume of slurry yielded a scaffold of 0.3cm height, a close approximation to the native TM.[10] Pores were induced with the aid of freeze-casting in a -80ºC freezer for roughly 30 minutes or until frozen through. Random, non-aligned pores were made as a result. This type of freeze casting was chosen as it was previously shown to produce the most mRNA protein expression in comparison to the aligned method or flash frozen with liquid nitrogen. These scaffolds were then lyophilized for 24 hours and crosslinked by a dehydrothermal mechanism in a vacuum oven at 105ºC under 29inHg vacuum for an additional 24 hours.[18] Soaking the finished scaffolds in 70% ethanol for several hours followed by a series of 2 rinses with PBS ensured sterility for cell culture studies.

2.3 Fabrication of Alginate-Chitosan Hydrogels

Both the chitosan and alginate polymers were manufactured in house from stocks of each. The alginate was purified by dialysis for 4 days, subjected to activated charcoal treatment, sterilized through a 0.22μm filter, frozen and lyophilized until dry. The RGD peptide was added prior to purification and allowed 20 hours to react with the alginate. The chitosan was formed using the stock supply of low molecular weight chitosan. The purification process was to combine chitosan with a 1% acetic acid solution (v/v) in a stirred 50ºC water bath for 18 hours to dissolve, where it was then filtered through progressively smaller filters of 22, 8 and 2.7μm. Dialysis was then performed for 4 days, before its pH was adjusted to 8.0 and it was lyophilized until dry.

The hydrogels were formed using stock solutions of 4wt% alginate or chitosan in PBS or 0.15wt% CS in PBS, a calcium sulfate slurry solution (210 mg/mL calcium sulfate in PBS), myoglobin, and TGFβ2. The stock solutions of the polymers were then either combined in a 1:1 ratio or a 3:1 ratio, resulting in 2:2wt% hydrogels or 3:1wt% alginate:chitosan respectively.

The calculated amount of each polymer was weighed within a sterile 3mL syringe (Becton Dickinson) before the corresponding amount of PBS or CS solution was added. A second syringe was then added using a luer lock adaptor to mix for approximately 30 seconds, or until the mixture was dissolved and homogenized. The desired amount of each polymer stock solution was then transferred into a new syringe, with 25μL of the calcium sulfate slurry per 0.5mL hydrogel added to one of the syringes before they were locked together and the three components were mixed for another 20 seconds. Depending on the experiment, myoglobin at 2mg/mL gel or TGF at 200ng/mL gel were added into the mixture as well. The slurry was then

measured out into 0.5mL increments into 1.5cm wells on a 24 well plate. Crosslinking occurred overnight in a humidified 37ºC incubator.

2.4 Rheology

Rheological measurements of the alginate-chitosan gels were determined using an AR-GR Rheometer attached to a 20mm crosshatched geometry set at a loading gap of 30,000μm. This loading gap space allowed for a fit of gels of 0.5mL distributed into each 1.5cm diameter well. Oscillatory strain sweep experiments were then run at a frequency of 1Hz by varying strain rate from 0.1% to 100% at 37ºC, with the loss and storage moduli recorded.[20] The stiffness of each hydrogel was taken as the value of the storage modulus at 1% strain, where N = 4 for each composition.

2.5 Hydrogel Release Studies and Bioresponse to TGFβ2 Exposure

The function of the alginate-chitosan hydrogels as extended drug delivery systems was tested through the use of myoglobin as a model protein. Myoglobin is a very common protein which is comparatively much easier to isolate and collect, making it more practical to use for testing the release system prior to introducing the TGFβ2. Expasy's tool for computing the isoelectric point and molecular weight of each protein was utilized, showing that myoglobin has a pI of around 7.1 with a MW of 17kDa, and TGFβ2 is 8.8 and 47kDa respectively.[42,43] The pair were thus considered a close enough estimate of one another to make the myoglobin release study a valid model. Albumin from bovine serum was also considered as it has a closer molecular weight of 69kDa, but its isoelectric point is approximately 5.8.[44] Due to this larger difference in the isoelectric point, which is generally more difficult to predict than molecular weight differences, it was eliminated as being the model protein.

The hydrogels for the myoglobin release study were prepared as described previously under non-sterile conditions. 2mg of myoglobin was added per mL of hydrogel mixture. Crosslinking occurred overnight in a humidified 37ºC incubator with a Millipore water soaked kimwipe placed between the plate and the cover to help prevent drying out. To begin the time of the release study, 0.5mL of PBS was added to each gel and then collected and replaced for all successive time points. The samples were then analyzed with the use of the Pierce™ BCA Protein Assay Kit using the standard protocol

2.6 Impact of Oxidative Stress in Cell Studies

In vitro cell studies were first performed on tissue culture plates in a traditional 2D manner to gather a baseline understanding of the expected impact. hTM cells were grown in flasks after being stored in liquid nitrogen at passage 2 before being pipetted into 24-well tissue culture plates covered in 0.1% gelatin in PBS for 15 minutes and rinsed with PBS. The cells were allowed to attach to the plates overnight, starved in serum free media the following 24 hours, then exposed to various concentrations of hydrogen peroxide the following day, for a total oxidative stress incubation time of 24 hours. This time was chosen as it was determined any longer amount of time would continue to kill off cells while 24 hours remained long enough to induce cell necrosis and begin cellular level change.

The studies were then expanded into the 3D network provided by the collagen scaffolds. Identical experiment conditions of serum starvation and peroxide exposure time were followed with the scaffolds. Previous studies highlighted that the number of cell attachment to the scaffolds was significantly reduced in comparison to those placed on tissue culture plates. To account for this difference, a direct comparison of the resulting data would not give an accurate portrayal, leading to the conversion of results into relative absorbance per environment type.

2.7 Antioxidant Investigation for TM Cells

As oxidative stress is a known contributing factor to apoptosis related with glaucoma, attention has also been focused on finding a suitable antioxidant for the disease. Three distinct antioxidants were trialed with hydrogen peroxide induced ROS stress in an attempt to find a novel therapeutic: resveratrol, CNPs, and peptain-1. The substances were introduced to the cell culture environments in two phases, termed preincubation and coincubation. 24 hours was allotted for the preincubation for the cells to take in the compounds in order to be prepared and use them once exposure to oxidation occurred. The coincubation period is referred to as the 24 hours where hydrogen peroxide was added, along with the presence of the potential antioxidant. This was done both with and without the presence of peroxide, where the former was intended to identify if there was any cell salvage from the oxidative stress, while the latter was to find if the compounds themselves were at all toxic to the cells.

The concentrations of each of the compounds were chosen based on previous experiments of concentration profiles conducted in the Krebs lab. For peptain-1, little was known about the peptide, so a full concentration profile was performed. Emphasis was placed on concentrations above 100ng/mL due to the findings of Professor Nagaraj at Anschutz.[34]

2.8 Quantitative Real Time Polymerase Chain Reaction with TGFβ2 Studies

mRNA levels were quantified via gene expression with qPCR following hTM cells cultured both on TC plates and CS scaffolds with TGFβ2 concentrations of 0 and 5ng/mL. Total RNA was isolated from each scaffold using the TRI reagent method.[45] The nucleic acid concentration and purity was then quantified using a Synergy H1microplate reader with a Take3microplate (Bio-Tek, Winooski, VT), with RNA reverse transcribed using a High-Capactiy cDNA Reverse Transcription Kit. Primers were designed using Primer Blast (NCBI, Bethesda,

MD), with pairs made for the genes of GADPH, collagen 1, fibronectin, and elastin (Table 2.1). The qPCR was run on a Roche LightCycler 480 instrument (Roche, Basel, Switzerland) with the Powerup SYBR Green Master Mix. Results were analyzed using the ΔΔCt method, where Ct shows the cycle number where the machinery is able to get a real signal from samples as they cross the threshold signal.

Table 2.1: Forward and reverse sequences of primers used for identifying gene expression with qPCR as designed with Primer Blast. All sequences are listed in the 5' to 3' manner.

Gene	Forward Primer	Reverse Primer
GADPH	ACC ACA GTC CAT GCC ATC AC	RCC ACC ACC CTG TTG CTG TA
Collagen 1	CAG CCC TGG TGA AAA TGG AG	GTG GGA CCA GGG GGC
Fibronectin	CAA AGC AAG CCC GGT TGT TA	CAA AGC AAG CCC GGT TGT TA
Elastin	TTC CCA GGT GGG GCC T	TTC TCC ACC AAG CAG TAG CA

2.9 Confocal Imaging of Cells and ECM Protein

hTM cells were cultured both on TC plates and CS scaffolds with TGFβ2 concentrations of 0, 5 and 10ng/mL. The media was then removed from each well, rinsed with PBS, and prepared for the confocal imaging. Each scaffold or well was fixed with 10% neutral buffer formalin for 15 minutes, before being permeabilized with 0.1% Triton X-100 in PBS and blocked with 1% goat serum for 15 minutes. All scaffolds except the negative control were then soaked in primary antibody elastin rabbit polyclonal IgG (1:400) overnight at 4ºC, followed by three rinses of PBS. Biotinylated secondary antibody goat anti-rabbit IgG (1:100) with 1% goat serum was then added to every scaffold to soak for 30 minutes at room temperature, then again rinsed 3 times with PBS. Finally, the scaffolds were soaked in streptavidin-CY3 (1:100) in PBS with 1% goat serum and DAPI (1:1000) for 30 minutes at room temperature, with 3 last rinses of

PBS. The scaffolds and tissue culture wells were visualized using a Leica microsystems DMi8 platform with 10x and approximately 9% grain.

2.10 Significance Analysis

Each experiment was performed with replicates of N = 4, with scaffold experiments having N = 4 + 1 for the negative control, from which the mean and standard deviation were thus calculated. These resulting data sets were compared with either 2-way or 1-way ANOVA to test for individual comparisons amid desired groupings (such as genes, scaffolds types, etc.). Differences among experimental groups were considered significant when $P<0.05$, represented by * in graphs. Increasing significance was shown with 2, 3, and 4 asterisks to demonstrate $P<0.01$, 0.001, and 0.0001 respectively.

CHAPTER THREE: RESULTS AND DISCUSSION

3.1 Oxidative Stress from Hydrogen Peroxide

As oxidative stress has been proven to be a factor in the cause of glaucoma, several experiments to investigate the role of oxidation in the traditional 2D cell culture plate against the more novel 3D collagen scaffolds were performed. Most impacts of ROS on cells eventually lead to apoptosis, so the desired reading from the cells was simply to see which remained viable after exposure to peroxide for a given amount of time. In order to gather such a reading, the CCK-8 assay was utilized, serving as a calorimetric assay to determine cell viability and proliferation in cytotoxicity studies. A water-soluble tetrazolium salt is reduced with dehydrogenase activities in cells to produce a yellow colored formazan dye, where the amount generated is directly proportional to the number of living cells by relying on NADH and NADPH activity.[46] Not only does it provide the amount of healthy cells, but it was also used as a means of normalizing oxidative stress results per cell number in the tissue culture environment.

When deciding the hydrogen peroxide concentration level and amount of time for exposure, several factors were taken into account. The general choices were to have a high amount of oxidation present for a short amount of time, or for a lower level to be present for a longer time point. The first option was chosen for the sake of faster experiments with more consistent results, with 24 hours of hydrogen peroxide introduced to the cell culture for a total of 24 hours. Preliminary experiments were conducted with time points of 24, 48, and 72 hours of peroxide exposure and high concentrations of hydrogen peroxide, choosing to follow the high and fast methodology (Figure 3.1). The hydrogen peroxide was diluted from the 30% stock in 3 serial dilutions, with the CCK-8 results as the data for the experiment.

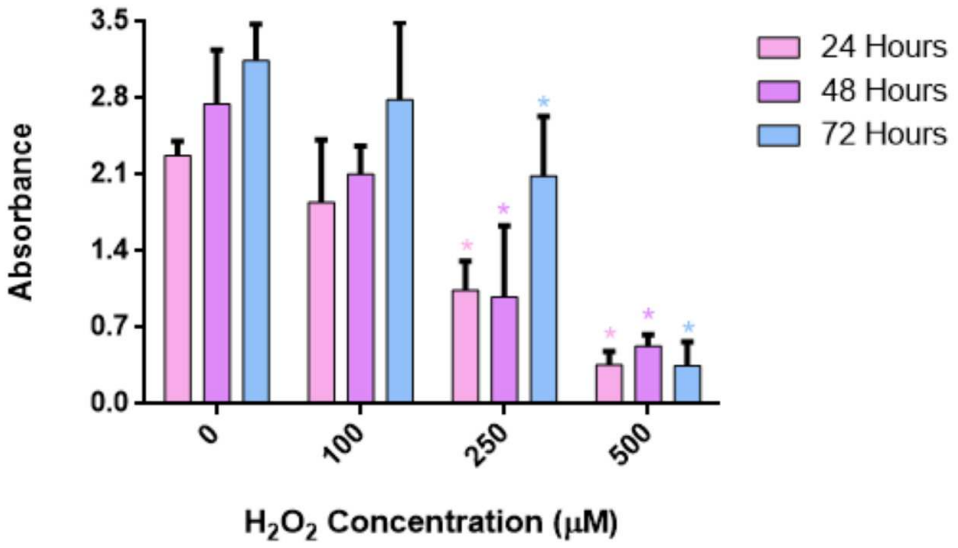

Figure 3.1: Relative cell activity from CCK-8 assay demonstrating cell survival with exposure to several concentrations of hydrogen peroxide for 3 time points with 50k cells seeded per well. * shows $P<0.05$ in relation to the 0μM concentration of the same time point. Absorbance was taken at 450nm.

The preliminary results showed that 24 hours provided enough time to see a significant difference in relative cell activity for 250 and 500μM. 48 and 72 hours also provided significance in the change between 0 versus 250 and 500μM, but were not ideal for several reasons. First, the 48-hour time point gave equal significance between both concentration relationships, and it was desired to have a clear distinction between the 250 and 500μM values. Second, the 72-hour time point showed with the increased value for the relative cell activity at 250μM that the cells appeared to have had time to recover from the oxidative stress, as there was an increased presence compared to the other two time points. Due to these factors, 24 hours of peroxide exposure was chosen to be the final time point for all continuing experiments, with the benefit of being a relatively quick time point to enable more experiments in the long run.

After the time point of 24 hours for the hydrogen peroxide exposure was determined, a detailed concentration profile study was carried out with hTM cells on tissue culture (TC) plates.

The intent was to find the relationship between relative cell activity and oxidation concentration, so that reasonable and applicable concentrations of peroxide could be reliably applied to cultures in future experiments (Figure 3.2).

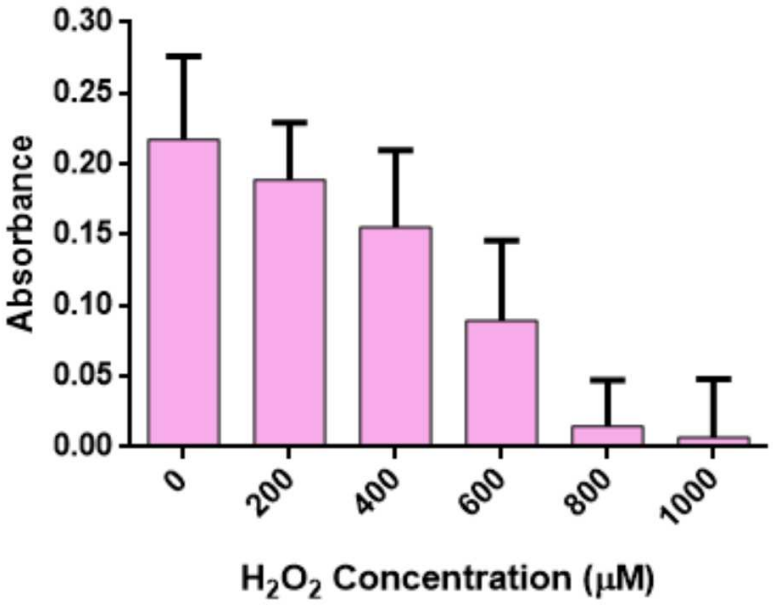

Figure 3.2: hTM cell exposure to peroxide at varying concentrations with relative cell activity from the CCK-8 assay. 20k cells were seeded in each well to avoid confluency with the assay performed after 24 hours, and absorbance recorded at 450nm.

The exposure of TM cells to progressively higher concentrations of hydrogen peroxide revealed a nearly linear downward trend of cell proliferation. The 500-700μM concentration was deemed the approximate halfway mark, where NADPH activity registered by the CCK-8 assay was missing in comparison to the healthy cell control. As such, this was chosen to be the concentration range for further oxidative stress studies. The half proliferation mark was desirable to be able to see any potential changes in cell response compared to the negative control, while still ensuring enough cell survival so as to be able to quantify the response.

Once the time point and hydrogen peroxide variables were determined from studies on traditional 2D cell culture environments, focus shifted to bringing in the 3D model of the collagen scaffolds. As research has shown oxidative stress is often a vital factor in people suffering from glaucoma, understanding the role of the microarchitecture and structure in a manner more related to the native TM was considered crucial. The 3D model enables more natural biosignaling and formation of the ECM, making it far more desirable for studies.

When proceeding to cell growth on the collagen scaffolds, several choices for the type of scaffold used were made. The original scaffold types were made using four different freeze casting techniques, either in -80ºC or with liquid nitrogen, and then aligned with the aid of a metal-bottom mold to achieve uniaxial heat transfer, or in an insulated mold to achieve random (nonaligned) pores. The nonaligned, -80ºC scaffolds were chosen for the conducted experiments reported in this paper. The nonaligned freezing method produced more consistent results, and the pore size were slightly larger than those frozen with the liquid nitrogen method, letting the cells migrate more easily within the 3D structure and have greater mRNA and protein expression. The finished result of the scaffold was a small white circle of 1.5cm in diameter and 0.3cm thickness, with a flexible and springy foam-like texture before being sterilized with ethanol. Once submerged in solution, the scaffolds become saturated and flaccid, although they still maintain their shape. Figure 3.3 shows a sample of the scaffolds.

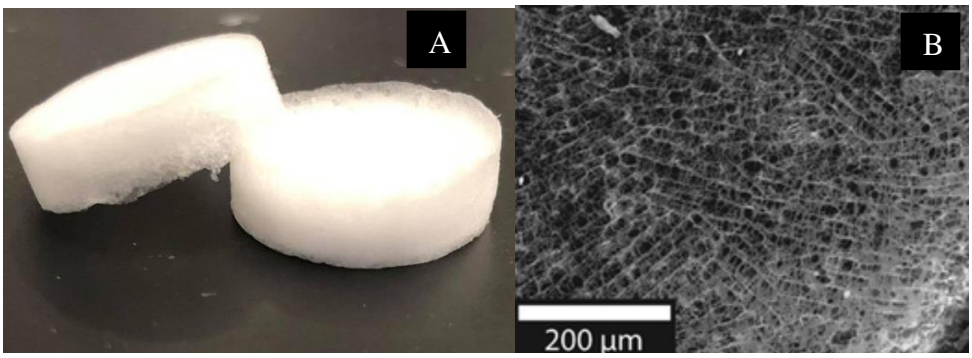

Figure 3.3A: A macroscopic view of the fabricated collagen CS scaffolds, showing their appearance as small foam-like disks about 1.5cm in diameter and 0.3mm tall. B: A scanning electron photo-micrograph showing the surface of the collagen CS scaffold with open pores.[19]

When recording cellular proliferation data using the CCK-8 kit, the samples cultured on TC plates provided different levels of signal than those cultured on collagen scaffolds, and therefore a study to ascertain what the differences were due to was undertaken. First, it was found that the blank values returned from the CCK-8 solution on its own in the presence of each scaffold composition were not statistically significant to one another or the solution by itself (Table 3.1). This means that the scaffolds themselves are not responsible for any differences observed in the absorbance assays. Therefore, the blank value can be taken as approximately 0.3 for all following CCK assays, demonstrating that any recorded values beyond that point are representative of cell NADPH activity and cellular life.

Table 3.1: Scaffold CCK-8 blank values by composition of added GAGs.

	Blank CCK Solution	CO Scaffold	CS Scaffold	HA Scaffold	CS/HA Scaffold
Average Absorbance Value	0.307	0.291	0.296	0.297	0.290
Standard Deviation	0.014	0.024	0.033	0.030	0.024

Additionally, the number of cells attaching to the tissue culture plate relative to the scaffolds was determined. Initial experiments showed a large gap in the CCK-8 values between

healthy cell control groups on TC versus scaffolds, which was either caused by a difference in the number of cells initially attaching or by different rates of proliferation. As the time point of 24 hours should not allow long enough for different proliferation rates to be of much impact, the cell attachment was assumed to be the source of the variance. As a result, an experiment was carried out to determine relative cell activity on tissue culture plates against scaffolds. The latter were pretreated in several ways to see if the cells would have higher attachment levels in a certain condition (i.e., when the scaffolds were soaked with media overnight or media was withheld to force greater contact between the cells and scaffolds initially).

The standard number of cells seeded onto TC plates and scaffolds was originally 50k, so this amount was placed onto TC plates treated with gelatin, as the standard procedure for TM cells. 50k cells were then placed onto scaffolds prepared for seeding with distinct media treatments, to find if the manner in which media was supplied was a source of importance. Previously cells were seeded onto scaffolds with the usual 0.5mL of media surrounding the structure, but the alternative methods of cell seeding onto a scaffold with no media, a scaffold rinsed with media, and a scaffold soaked in media overnight were studied. 4 hours is the minimum time required for cells to form attachments to a new environment, so the CCK assay was conducted at this time point to avoid allowing the cells additional time to proliferate and confound the data (Figure 3.4). A cell seeding amount of 75k was also studied for the scaffolds to try and bridge the gap of the smaller amount which attach to them in comparison to the TC plates. 75k seeding was not conducted on the tissue culture plates themselves as it would overwhelm the growth space and instantly become confluent, making it so not all cells would find a location to attach and skewing the interpretation of the data.

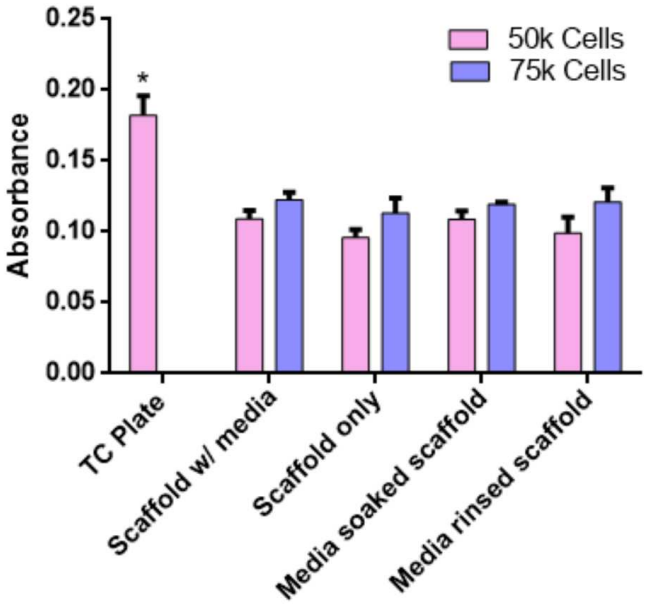

Figure 3.4: Relative cell number results using the CCK-8 assay as recorded at 450 nm. Different cell seeding conditions were investigated using two cell concentrations of 50 and 75k after 4 hours for attachment. The blank value of the CCK solution on its own was subtracted, so all values present represent cell activity. 50k on TC plate is significant from all other values with * $P<0.05$.

The results from the scaffold seeding experiment highlighted that the seeding of 50k cells on TC plate is statistically significant from all types of cell seeding onto scaffolds with both 50k or 75k cells. This confirms that when comparing cell responses to oxidative stress, the assay results must either be normalized to the number of cells per individual well or to the type of culture environment for a fold change.

Next, to induce oxidative stress in the TM cells, hydrogen peroxide and TGFβ2 were added to the media surrounding the scaffolds. 700μM hydrogen peroxide was chosen based on the results from Figure 1, as it was expected to see a dramatic change in cell activity with more than half of the absorbance value depleted. The TGFβ2 concentration was selected as 10ng/mL, reaching the upper limit of the expected concentration found in the aqueous humor of POAG patients, once again meant to trigger a noticeable response. The CCK-8 assay results are shown

in Figure 3.5, where the 24-hour time point of exposure was maintained from previous experiments.

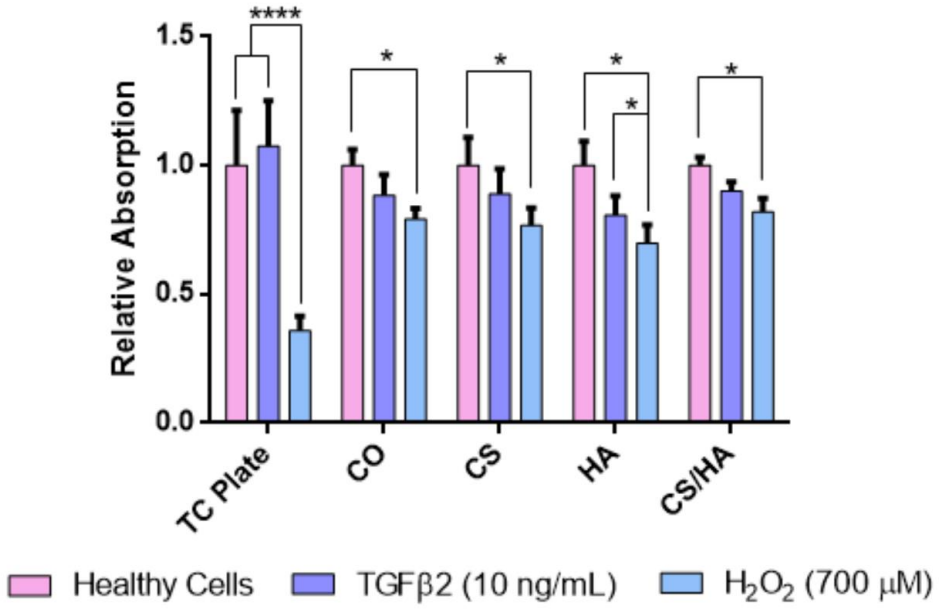

Figure 3.5: Fold change results of relative activity for hTM cells under exposure to hydrogen peroxide and TGFβ2 on TC plate and collagen scaffolds. CCK-8 asssay was collected at 450nm. * shows P<0.05 significance with **** showing P<0.0001.

When moving the oxidative stress studies to the 3D environment provided by the collagen scaffolds, several trends became apparent. The first and most important takeaway was the impact the scaffolds had at reducing cell death in the presence of hydrogen peroxide. At the concentration of 700μM, the relative absorption on the TC plate from healthy cells to those in peroxide was 1.0 to 0.36, showing a significance of P<0.0001. In contrast, the fold change of healthy cells on scaffolds to peroxide exposed cells on scaffolds was 1.0 to a range of 0.82 to 0.70, depending on scaffold type. While still significant, the relative absorption change was drastically less than that of TC plates, with a P value of <0.05 for the scaffolds.

These results provide conclusive evidence that in these conditions, the 3D model the scaffold provides for the culture of TM cells allows the cells to be more resistant to the effects of oxidative stress. The direct implication for glaucoma research as a whole is how vital it is to have the correct 3D environment for *in vitro* studies relating to the trabecular meshwork. The porous structure of the collagen scaffolds enables the cells to more closely mimic the native TM environment, giving researchers a better understanding of how cells respond *in vivo*. The architecture allows for their signaling and proliferation to be far more natural than a simple 2D culture. Studies performed with oxidative stress, antioxidants, and other drugs on 2D cell culture systems could prove highly inaccurate. The TM cells in this study were drastically more impacted by oxidative stress in the 2D culture, meaning that similar studies to find therapeutics for glaucoma could easily yield false results. The 2D culture could suggest an important cell response to whatever drug was introduced, whereas in reality the 3D nature of the trabecular meshwork is so complex and integrated the cells will have different levels of response in this format. A promising therapeutic or discovery in 2D environments could thus prove meaningless when it came to the realistic 3D nature of the eye.

The second implication of the study from Figure 4 is the lack of significance between the healthy cells and the ones exposed to TGF in any of the environments. Neither the TC plate nor the four scaffold types produced a change in relative cell activity large enough to be marked by the CCK-8 assay. For this reason, attention was instead turned to a gene expression level to determine 3D environmental effects resulting from the cytokine's presence.

3.2 TGFβ2 Exposure and Gene Expressions on Scaffolds

As previously discussed, TGFβ2 is a powerful cytokine primarily known as a profibrogenic agent. While it does have direct impacts on the amount of ROS present in the

environment, more immediate effects can be seen with the gene expression levels of fibrotic proteins.[47] When using TGFβ2, it has been found that at least 24 hours of exposure are required in order to see increased expression levels of collagen 1, so this was taken as being the very minimum option for experiments.[48] As the Cp value was seen to decrease – making it more desirable for accurately detecting gene expression levels – when the length of the experiments was increased, the chosen time point was 72 hours before RNA isolation was begun.

Samples of healthy cells, those exposed to 5ng/mL and 10ng/mL TGFβ2 were cultured on tissue culture plates in the typical manner and then on the collagen scaffolds for modeling the 3D environment. Only the CS type scaffolds were used as little significance was found with scaffolds enriched with GAGs in the hydrogen peroxide experiments. Media was changed every other day, before RNA isolation and cDNA conversion was performed. qPCR was then run with GAPDH as the housekeeping gene, and the fold changes found from the samples are reported in Figure 3.6. Three fibrotic proteins were run to determine amounts of mRNA from gene expression, including collagen 1, fibronectin, and elastin.

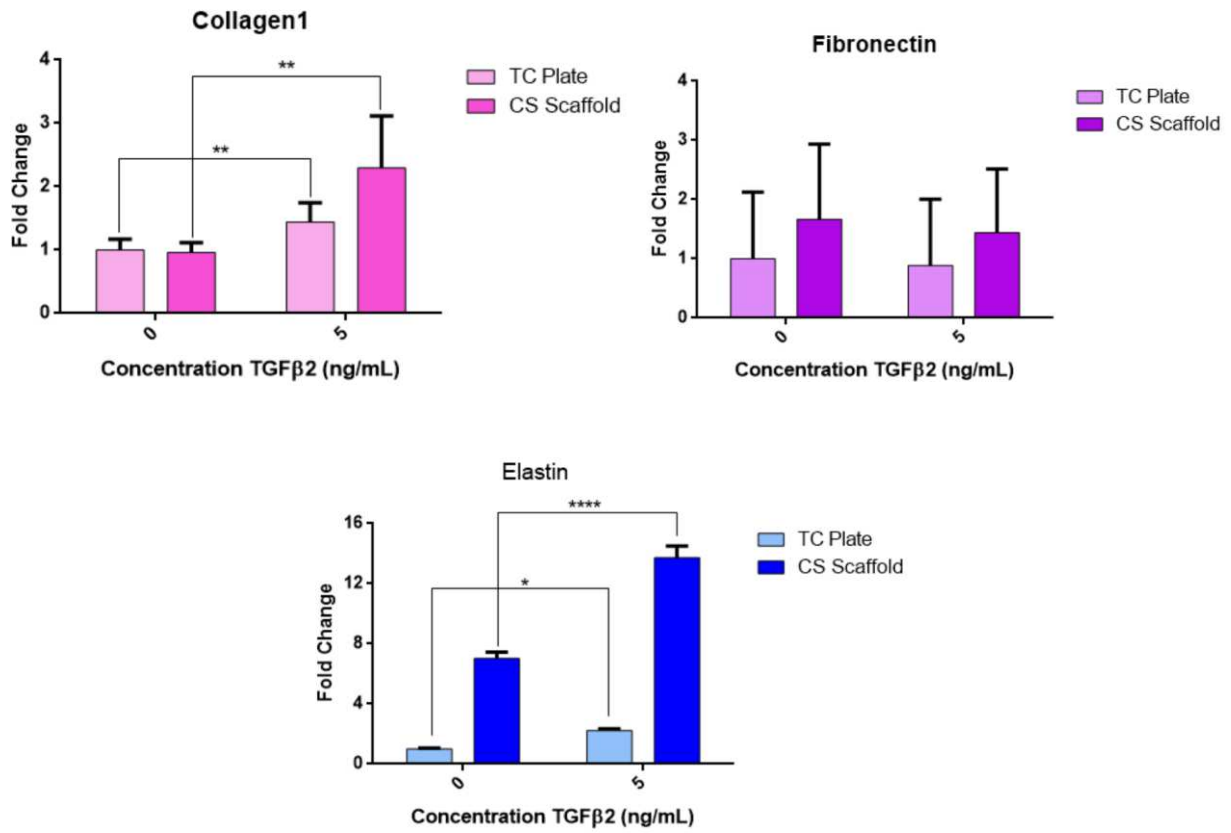

Figure 3.6: qPCR results from TGFβ2 experiment conducted to compare TC plate to collagen scaffold environments in relation to mRNA expression of fibrotic protein genes. Statistical significance is shown where * is P<0.05, ** is P<0.001, and **** is P<0.0001.

The qPCR results had several points of significance between the cells exposed to 5ng/mL TGFβ2 and those with none. Fibronectin was the only investigated mRNA found to not undergo an increase in expression with the introduced cytokine, although the relatively large standard deviations make this impossible to claim with significance. Collagen 1 had nearly identical results for fold change between the TC plate and CS scaffold, going from 1.0 to 1.4 and 0.96 to 2.3, respectively.

The point of the most importance was found with the elastin gene. As a major constituent of the ECM in the trabecular meshwork, it was expected for elastin (and all other fibrotic mRNA) expression to increase with the profibrotic TGFβ2. This trend was found on both the TC

plate and the scaffolds, but with drastically different magnitudes. The change of 1.0 to 2.2 versus 7.0 to 13.7 demonstrates how vital the 3D environment may prove to be in the culturing of hTM cells. The elastin presence was 7-fold higher than that of the TC plate in the CS scaffold without any TGFβ2 exposure, showing how the additional microstructure and biosignaling enabled by the 3D scaffold can impact data for *in vitro* studies. Furthermore, the increase with the cytokine expression was approximately 6-times that of the increase for TC when compared to the scaffolds. This experiment demonstrated that while tissue culture plates may provide the overall correct trend of mRNA expression of fibrotic proteins, it is sorely lacking at times when it comes to the magnitude of these changes, which could easily produce false results when it came to testing cell response to oxidative or therapeutic agents.

As an additional qualitative data analysis, images of the scaffolds and tissue culture plate were also taken using confocal microscopy. The environments were stained for detecting the nucleus using DAPI and the protein elastin in the extracellular matrix with rabbit antibodies (Figure 3.7).

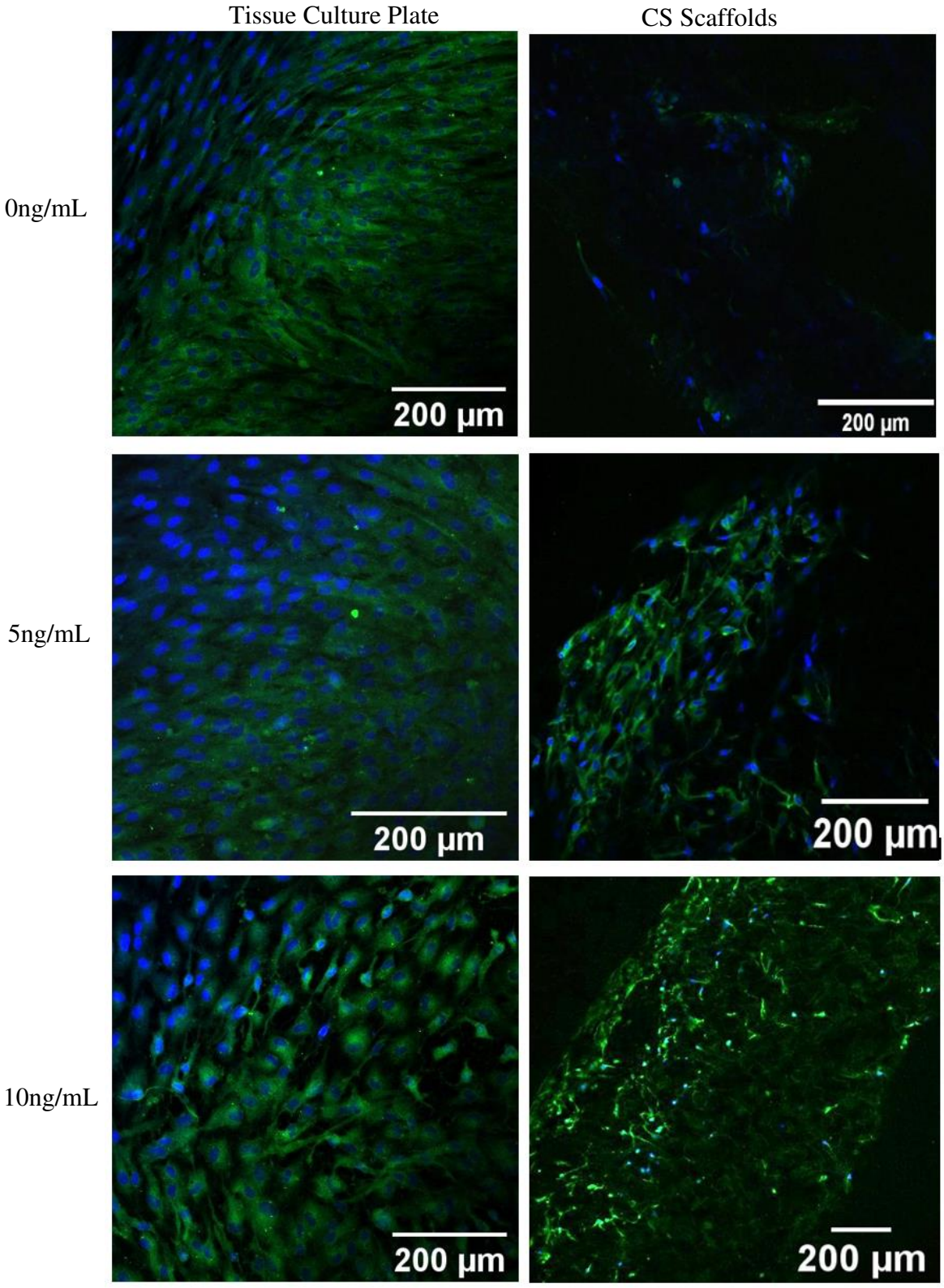

Figure 3.7: Confocal images with elastin staining performed with a Leica DMi8 microscope, approximately 9% grain at 10x, with the cell nucleus stained with DAPI shown in blue and the elastin stained with its antibody stained with CY3 shown in green.

The images taken with the confocal microscope confirm the numerical results from the qPCR studies, proving that the patterns of mRNA levels in the cells are following through to protein expressions in the ECM. The hTM cells exposed to TGFβ2 on the CS scaffolds produced a noticeable increase in the amount of elastin in the ECM, as can be seen by the higher amounts of green staining in the 5 and 10ng/mL pictures respectively. The same trend is visible in the tissue culture grown cells as well, although the elastin has less distinct structure without the architecture provided by the 3D scaffold. Both sets of images support the data found with gene expression analysis, while also highlighting the structural differences in the ECM when the hTM cells are given a biomimetic model to grow on.

3.3 Hydrogel Rheology, Release Studies, and Cell Culture Viability

While the collagen scaffolds provided an excellent microarchitectural environment to mimic the native trabecular meshwork, it was desired to expand upon this. Not only would it be beneficial for the TM cells to grow in a 3D structure to allow for their characteristic biological signaling and ECM deposition, but the ability to introduce a drug into the culture slowly over time would continue to make the model more effective. Glaucoma is generally a chronic condition, taking years to progress to the point that symptoms are noticeable and the individual will seek medical help.[49] Cell culture studies where TM cells are induced to a glaucoma like state (whether through the use of dexamethasone or other reagents) are normally conducted by introducing a high concentration of the stress into the environment at a single time. In reality, glaucoma conditions of high levels of oxidative stress or TGFβ2 certainly do not take place overnight, but over a period of weeks, months, or years.

To combine the structural accuracy of the 3D *in vitro* model with the drug delivery capabilities reflected in the disease of glaucoma, hydrogels were investigated. Alginate-chitosan

crosslinked polymers are a well-studied reaction, where the stiffness of the gels is found to increase with the presence of the cation calcium. When a reagent is incorporated into the slurry while mixing the polymers, it will release slowly into the surrounding culture over time.

To begin, it was first desired to confirm that the hydrogels could accurately reflect the stiffness of the native TM, as a 3D model with no flexibility or which could not hold its shape over time would prove meaningless. The stiffness of the native TM has a wide range in humans, accepted to be anywhere from 1.7 to 8.8kPa in healthy eyes. The range considered normal for those with glaucoma does not begin until 80kPa, leaving a wide gap between the two as a grey area.[50]

Four different compositions were chosen for the hydrogels based on this data: a ratio of 2:2 wt% and 3:1wt% alginate:chitosan, with and without the presence of CS. The amounts made it possible to get the polymers into solution with only a few minutes of mixing, and the altered ratio to have a higher proportion of alginate was intended to impact the release studies. CS was additionally added to half of the gels as well, as it is a GAG present in the TM known for its antioxidant properties, with its inclusion also helping to better mimic the native eye.[51] The hydrogels were then put through rheological testing (Figure 3.8). A variation of the gels containing myoglobin was also run, serving to answer how the addition of the model protein would alter the mechanical properties. Images of the hydrogels directly after crosslinking are provided in Figure 3.9.

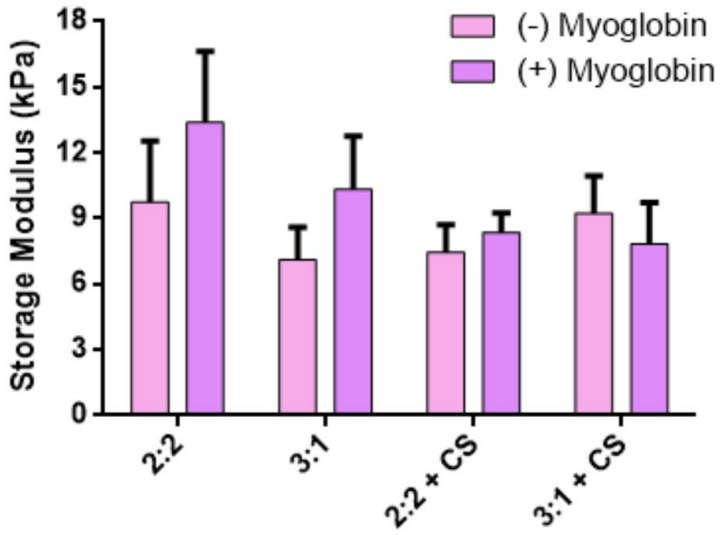

Figure 3.8: Rheology results for the storage modulus at 1% strain of alginate-chitosan hydrogels, serving as an estimate of material stiffness. None of the hydrogel types had any statistical significance when compared between the with and without myoglobin samples.

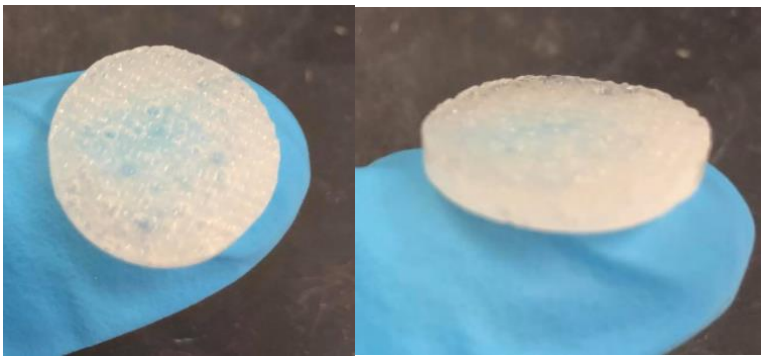

Figure 3.9: Macroscopic images of the the fabricated hydrogels (2:2wt% alginate:chitosan). The finished product was ~1.5cm in diameter and 0.25mm high, with both a side and overhead view. The images were taken with the PEC placed on a fingertip for scale.

The results of the rheology testing indicate that the stiffness of the hydrogel compositions selected all fall within or near the range of accepted normal human eye stiffness. Of the 8 gels tested, the range of stiffness ran from 7.1 to 13.4kPa, making them a reasonable estimate of the native TM and ensuring they would retain their structural integrity over the course of several days or weeks in solution. There was no significant difference found in the stiffness either

between pairs of gels with the same composition with or without myoglobin (between each pair of pink and purple bars) or across any of the four gels (all of the pink or all of the purple). This demonstrated no clear preference for which of the gels would best represent the TM, so all were investigated moving forward.

After the stiffness properties of the hydrogels were confirmed to fall within accepted values for the trabecular meshwork, attention was turned to modeling drug release abilities. As discussed, the model protein myoglobin was chosen and integrated within the PECs while mixing the slurry. The Pierce™ BCA Protein Assay Kit was used to measure the levels of protein taken from each time point sample of PBS surrounding the hydrogels. The calorimetric detection and quantification of the total protein relies on comparing the absorbance values to those generated by a standard curve made with bovine serum albumin. The assay combines the reduction of copper with the sensitive and selective detection of the resulting ion. Color formation is dependent on the structure and size of the protein, in addition to the number of four specific amino acids: cysteine, cystine, tryptophan and tyrosine.[52] The conversion of absorbance value to protein level was calculated with the standard, producing the release curve (Figure 3.10) as a percentage of total myoglobin released over time.

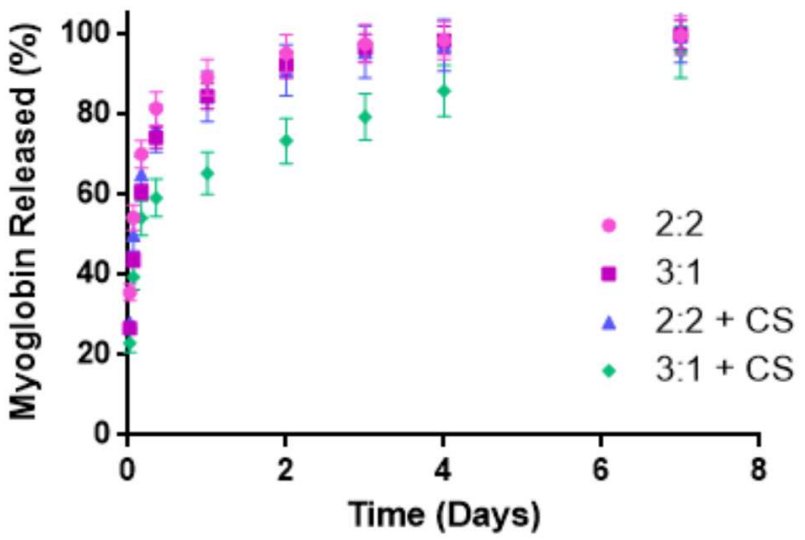

Figure 3.10: Release model of myoglobin from alginate-chitosan hydrogels. The weight percentages of each gel are listed as ratios.

The release study performed with myoglobin demonstrated the successful release of the protein from the four different PEC compositions over time. Approximately 95% of the incorporated myoglobin was released into the surrounding PBS after a week of the start of the study. Comparing the different compositions of the hydrogels, two trends can be seen. First, the 2:2wt% mixture had the fastest release, giving off 35% of the total myoglobin in the first 30 minutes, and 89% in the first 24 hours. The 3:1wt% gel had a slower initial release, with only 27% excretion in 30 minutes and 84% in 24 hours. This slightly delayed release is expected, as the increased ratio of alginate present in the slurry provides more gelation with the added calcium cation. Following this trend, the protein release from any gel with a higher wt% of alginate should lead to an increase in the time it takes to deliver the protein.

The second trend present from the study is that the addition of the 0.15wt% CS to the hydrogel causes a slower myoglobin release in comparison to its same weight counterpart in PBS. The 2:2 + CS and 3:1 +CS wt.% gels had release percentages at 30 minutes and 24 hours of

24% and 84%, and 23% and 65% respectively. This shows the decreased delivery of the protein when CS is incorporated into the matrix, while still following the first trend of the larger alginate presence slowing down release as well. All four compositions successfully released almost all of their myoglobin into their environment, proving these specific compositions can support drug delivery, at least of those structures closely related to the myoglobin model. Due to the higher molecular weight of the TGFβ2, it would be expected that the release curves followed the same general pattern and shape but with an extended x-axis, as it would take longer for the bigger structure to go through mass transfer.

Once the hydrogels were proven to have similar stiffness to the native trabecular meshwork and functionality as drug delivery systems, it was finally investigated whether or not they would be able to promote attachment to hTM cells and thus serve as a full 3D model for cell culture. To explore this, the four gel compositions were made in sterile conditions, before being treated with ethanol and UV light to further prevent contamination. 50k cells were seeded and allowed to grow for 48 hours to prove cell attachment, with viability measured with the CCK-8 assay (Figure 3.11). Prior to adding the calorimetric solution, the hydrogels were moved to a fresh TC plate, so that the CCK-8 readings could be interpreted for cells attached to the gel as desired and those which sank through to the TC plate itself.

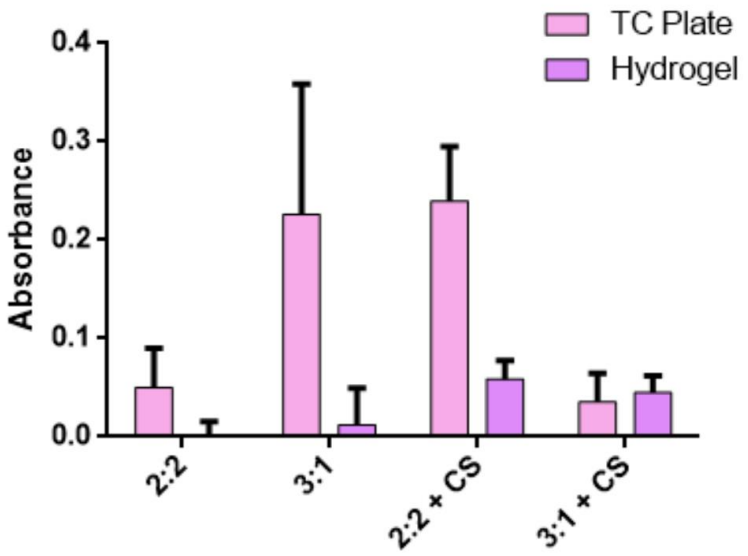

Figure 3.11: Relative cell activity provided by the CCK-8 assay at an absorbance of 450nm to determine cell attachment to the four compositions of hydrogels or to the bottom of the TC plate 2 days after seeding.

Based on the above results, the majority of the cells seeded onto the hydrogels are in actuality sinking to the bottom of the tissue culture plate and attaching there instead of to the physical gel. As the cells are still alive, it proves that the PECs would be a viable method of delivering drugs to hTM cells in a sustained manner. However, it would be more ideal to have the cells attached to the hydrogels themselves, thus providing them the 3D structural framework which is crucial for a more accurate model. The presence of CS in the slurries made an impact on improving cell attachment to the gels, meaning that to improve the results, the wt% of CS in the mixture could be increased, along with the amount of RGD motif added to the alginate when purifying the polymer. This would hopefully ensure good cell attachment to make the gels both a drug delivery system and a 3D culture environment.

3.4 Antioxidant Studies

After the in-depth studies of oxidative stress in hTM cells on both 2D and 3D structures, there was a desire to try and identify a novel therapeutic with promising antioxidative properties. As discussed, resveratrol, CNPs, and peptain-1 were the 3 identified compounds of interest, either due to known antioxidant abilities, reactive oxygen and nitrogen species scavenging, or neuroprotection against apoptosis. Each of the three was studied individually, using a timeline of seeding the cells on TC plates, allowing them to sit for 24 hours in what is called the preincubation period, then continuing a second 24 hours in the coincubation period. The two types of incubation refer to whether or not the cells were given the antioxidant. In order for the cells to be able to use the antioxidant against the hydrogen peroxide induced ROS stress, time was given for the cells to take in the drug before the introduction of the peroxide. In this manner, the cells were equipped with the compound in advance of the oxidative stress, theoretically allowing them to better withstand the exposure. TM cells were given either one or two doses of the antioxidant (coincubation, or preincubation and coincubation together), with one set of samples exposed to peroxide to determine ROS salvaging abilities and one set not given peroxide to determine potential toxicity of the agent to the cells.

This study was performed with identical environments with both resveratrol and CNPs (Figures 3.12 and 3.13). 250μM hydrogen peroxide was selected as the concentration for these studies in order to see a discernible change between the healthy cell and peroxide controls, while not inducing extreme amounts of cell death so the amount of antioxidants could be kept to a minimum. RSV concentration was kept constant at 1μM, with CNPs at 10μM, based on previous concentration studies performed within the lab group.

While the CCK-8 assay was run to determine relative cell activity numbers and thus show if cell salvaging or death from toxicity occurred, an assay for calculating ROS was also introduced. Known as the H2DCFDA – Cellular ROS Assay, the protocol is dependent on the diffusion of the fluorogenic dye into the cell. It is then deacetylated by cellular esterases to a non-fluorescent compound, which is then oxidized by ROS (including hydroxyl, peroxyl and others) into DCF, which is highly fluorescent.[53] Each reading was normalized to the relative number of cells provided by the CCK-8 assay.

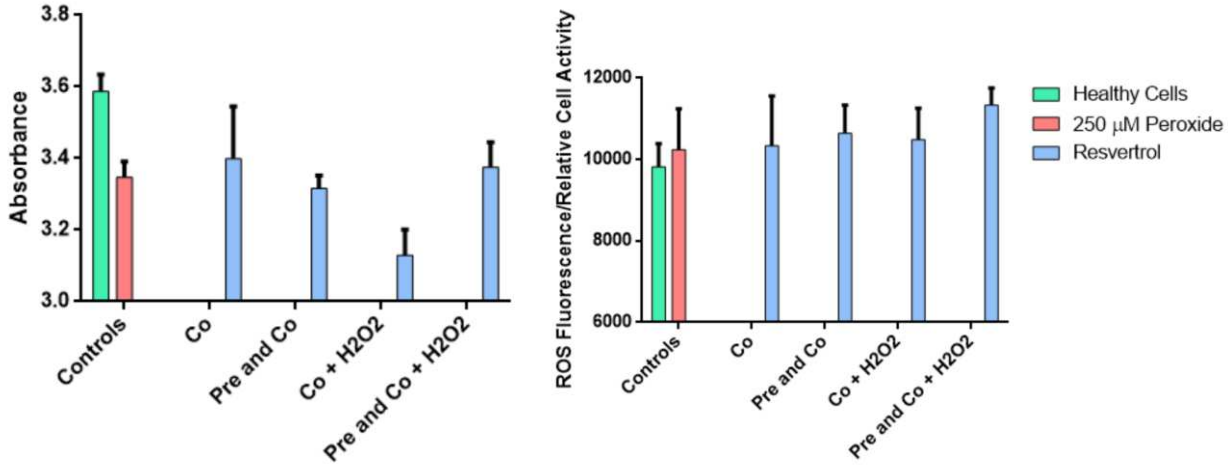

Figure 3.12: Relative cell activity data provided by the CCK-8 assay and ROS H2DCFDA assay for testing the efficacy of resveratrol as an antioxidant for TM cells. Preincubation and coincubation of RSV lasted 24 hours each, with hydrogen peroxide added only during the latter. Absorbance was taken at 450nm for CCK-8, with 490nm and 520nm for the excitation and emission of the ROS protocol.

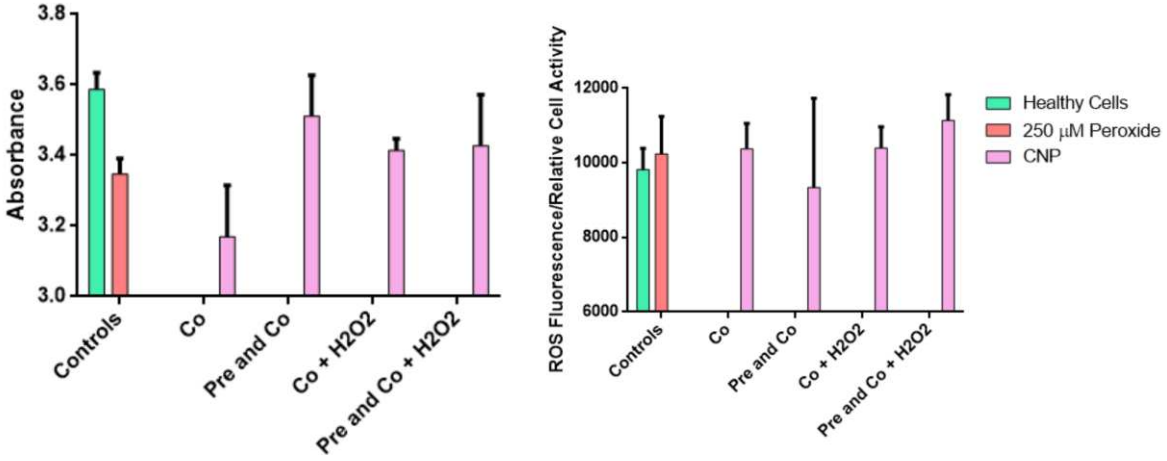

Figure 3.13: Relative cell activity data provided by the CCK-8 assay and ROS H2DCFDA assay for testing the efficacy of CNPs as an antioxidant for TM cells. Preincubation and coincubation of RSV lasted 24 hours each, with hydrogen peroxide added only during the latter. Absorbance was taken at 450nm for CCK-8, with 490nm and 520nm for the excitation and emission of the ROS protocol.

After the CCK-8 assay, it was found that the RSV might have enabled a small amount of cell rescue from hydrogen peroxide when placed through both preincubation and coincubation, despite the fact that the same treatment without peroxide appears mildly toxic to the cells. A similar observation was made for CNPs, with the coincubation alone producing the same trend. Furthermore, the ROS assay gave somewhat inconclusive results, with the standard deviation error hindering the ability to make any significant claims. Further testing with different concentration profiles was planned for the future, with attention turned to the third and final potential antioxidant.

After work with RSV and CNPs revealed that preincubation appears more vital to antioxidant functions over coincubation, it was decided to focus only on the first when it came to studying peptain-1. As it was the least researched antioxidant by other groups, the most attention was given to it out of the three, with a full concentration profile experiment conducted. A collection of samples was run both with and without peroxide – again to test for toxicity to the

cells with the peptain-1 on its own – with 24 hours for preincubation of the peptain-1 into the cells and then 24 hours of exposure to hydrogen peroxide to induce oxidative stress. The concentration of the peroxide was selected as 500μM, with relative cell activity determined using the CCK-8 assay (Figure 3.14).

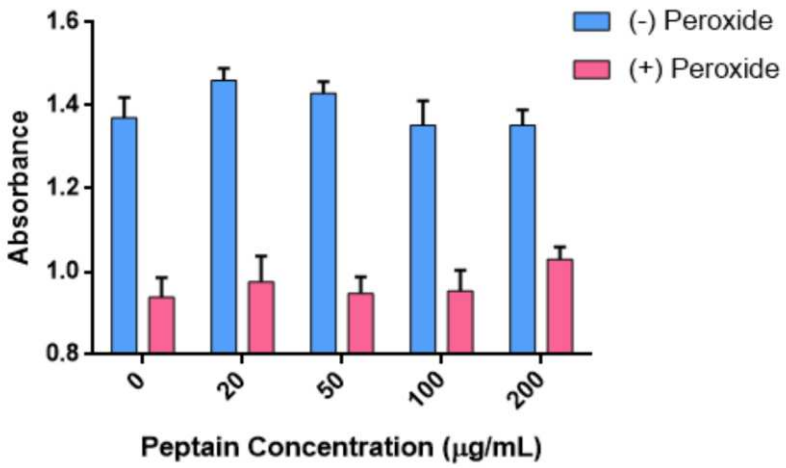

Figure 3.14: Relative cell activity data provided by the CCK-8 assay for the peptain-1 concentration profile and antioxidant potential experiment when exposed to 500μM hydrogen peroxide. Absorbance for the assay was taken at 450nm.

To accurately account for the antioxidant properties of peptain-1, each of the CCK-8 values for the samples exposed to peroxide was normalized to the values of samples without peroxide (pink divided by blue bar for each concentration pairing). The results are shown below (Figure 3.15) where the normalization was able to produce significant results whereas the non-normalized data had no significance among any of the with or without peroxide groupings (among just pink or just blue).

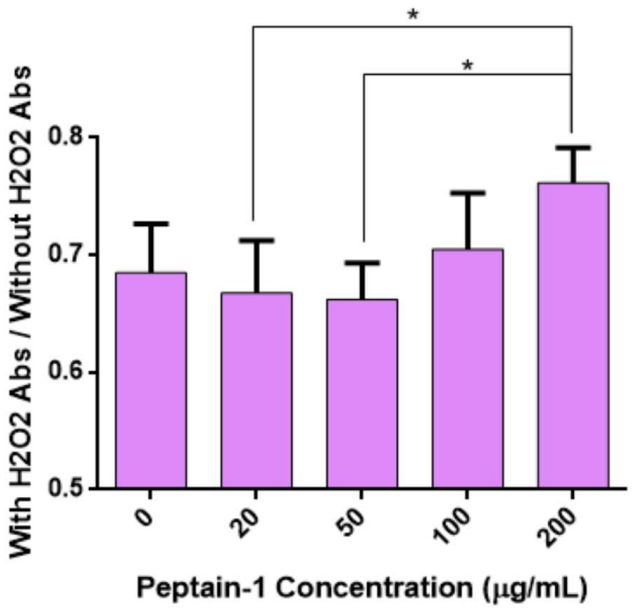

Figure 3.15: CCK-8 assay results showing relative cell activity of hTM cells exposed to hydrogen peroxide normalized to those not exposed. Both were treated with varying concentrations of peptain-1 to study antioxidant and toxicity effects, where * shows $P<0.05$.

The normalization of the peptain-1 trials with peroxide to the corresponding ones without peroxide revealed two points of significance. The concentration of 200μg/mL against both 20 and 50μg was significant with $P<0.05$. This experiment used the remainder of the peptain-1 the lab was provided, but an additional point of significance would likely exist between 0 and 200μg/mL concentrations if the study were repeated and the error bars were lessened. These significance results highlight that peptain-1 could be a potential antioxidant therapeutic once it has been administered in 200μg/mL concentration, serving to rescue a noticeable number of cells from ROS stress.

CHAPTER FOUR: SUMMARY

4.1 Summary of Results

During the course of this research, we expanded upon previous work in the Krebs lab in order to determine the impact a more nature 3D model of the trabecular meshwork has on TM cells exposed to oxidative stress. This was conducted using two distinct culture environments, with the first being collagen scaffold based. These freeze-casted scaffolds provide microarchitecture which closely mimics that of the native TM, encouraging cell migration and proliferation throughout. These scaffolds significantly lessened the damage wrought by oxidative stress induced by hydrogen peroxide in comparison to cells cultured in the traditional 2D manner, highlighting the important role the biosignaling and ECM play in maintaining cell health which cannot be reflected properly on tissue culture plates. Additionally, it was found that the profibrotic cytokine TGFβ2 had several insightful trends on TC plates versus on scaffolds. Fibronectin and elastin revealed nearly identical constant expression and significantly increased, respectively. However, collagen 1 demonstrated a nearly twofold increase on scaffolds in comparison to tissue culture samples, highlighting the importance of the 3D microenvironment and how it may play a pivotal role in cell response.

The second major system investigated was that of hydrogels composed of alginate and chitosan, with four different compositions serving to change the rate of release with the protein model myoglobin. The successful release of approximately 99% of the protein over the course of a week, along with the stiffness falling within the accepted range of the trabecular meshwork in human eyes, leads the PECs to be a viable environment for TM cell study. Experiments proved

that while some cells were attaching to the gels, there was much room for improvement, which could be brought about by increasing RGD motifs in the alginate polymer or with increased levels of CS.

The antioxidant studies showed promise in the development of the two novel therapeutics of CNPs and peptain-1, although there were not sufficient findings to make any definitive claims. However, several points of preincubation with the two agents demonstrated what has potential cell rescue in the presence of hydrogen peroxide,

4.2 Future Works

The nature of the research performed leads to the question of finding suitable antioxidants to help reduce oxidative stress which occurs naturally in the trabecular meshwork and thus reducing the potential damage leading to glaucoma or other eye diseases. Three such antioxidants were explored during this research: resveratrol, CNPs, and peptain-1. None of them were found to work perfectly in the concentrations used, but the peptain-1 and CNPs showed promise.

After the success of the myoglobin model, the release of TGFβ2 should be investigated in the alginate-chitosan hydrogels. A two-week release study was performed, but the amount of protein expected to be in the collected solution was so small as to make the BCA kit or microBCA kit unable to be used. An ELISA assay must be performed to analyze the collected data to make the release curve, after which point cells may be introduced to the environment with their ROS and relative cell activity studied in against cultures where all the TGFβ2 is introduced at once.

For the hydrogels, it would be ideal to ensure more reliable attachment of cells to the gels itself rather than the TC plate below. This would provide a 3D environment for the cells to better

mimic the native TM, along with providing a drug delivery system. The protein myoglobin could be exchanged for not only TGFβ2, but also numerous other oxidative stress agents or antioxidants. The peptain-1 might prove a unique opportunity for the hydrogel release, as it was found that a relatively high spike of the compound is needed to see any cell rescue, which would be instigated by the PECs before tapering off to a more moderate release.

4.3 Conclusion

This thesis details the culmination of the work performed in analyzing two 3D model environments for use in culture of human trabecular meshwork cells. The collagen scaffold *in vitro* models demonstrated key differences from the tissue culture models, resulting in increased oxidative stress resistance and a greater response to TGFβ2 with the increased production of collagen 1. Alginate-chitosan gels of four different compositions had stiffness similar to the native TM while simultaneously releasing the model protein myoglobin into the surrounding solution, with cell attachment showing the gels may be a viable 3D model with the drug delivery system. Finally, antioxidant work led to a better understanding of two novel agents – peptain-1 and CNPs. Future work should include working on better cell attachment to the hydrogels and studies of different drugs incorporated into the matrix, such as TGFβ2 for oxidative stress induction or peptain-1 as an antioxidant presence. Additionally, the collagen scaffolds reveal a more accurate model to the TM over tissue culture plates, with their unique cell responses demonstrating the importance of using these biomimetic structures.

REFERENCES

1. CDC. Don't Let Glaucoma Steal Your Sight! *Centers for Disease Control and Prevention* https://www.cdc.gov/visionhealth/resources/features/glaucoma-awareness.html (2020).

2. Cataracts | National Eye Institute. https://www.nei.nih.gov/learn-about-eye-health/eye-conditions-and-diseases/cataracts.

3. Glaucoma the 'Silent Thief' begins to tell its Secrets. *National Eye Institute* https://www.nei.nih.gov/about/news-and-events/news/glaucoma-silent-thief-begins-tell-its-secrets#:~:text=Glaucoma%20is%20sometimes%20called%20the,there%20is%20any%20vision%20loss. (2014).

4. Español, I. en, Statement, A., Policy, P., Use, T. & C. of & Credits, P. Understand Your Glaucoma Diagnosis. *Glaucoma Research Foundation* https://www.glaucoma.org/treatment/understand-your-glaucoma-diagnosis.php.

5. Glaucoma - Symptoms and causes. *Mayo Clinic* https://www.mayoclinic.org/diseases-conditions/glaucoma/symptoms-causes/syc-20372839.

6. Emory Eye Center | Ophthalmology Terms. http://www.eyecenter.emory.edu/ophthalmology_terms.htm.

7. Mahabadi, N., Foris, L. A. & Tripathy, K. Open Angle Glaucoma. in *StatPearls* (StatPearls Publishing, 2021).

8. Beidoe, G. & Mousa, S. A. Current primary open-angle glaucoma treatments and future directions. *Clin. Ophthalmol. Auckl. NZ* **6**, 1699–1707 (2012).

9. Español, I. en, Statement, A., Policy, P., Use, T. & C. of & Credits, P. Symptoms of Angle-Closure Glaucoma. *Glaucoma Research Foundation* https://www.glaucoma.org/glaucoma/symptoms-of-angle-closure-glaucoma.php.

10. Abu-Hassan, D. W., Acott, T. S. & Kelley, M. J. The Trabecular Meshwork: A Basic Review of Form and Function. *J. Ocul. Biol.* **2**, (2014).

11. Gonzalez, J. M., Hamm-Alvarez, S. & Tan, J. C. H. Analyzing Live Cellularity in the Human Trabecular Meshwork. *Invest. Ophthalmol. Vis. Sci.* **54**, 1039–1047 (2013).

12. Torrejon, K. Y. *et al.* Recreating a human trabecular meshwork outflow system on microfabricated porous structures. *Biotechnol. Bioeng.* **110**, 3205–3218 (2013).

13. Dautriche, C. N. *et al.* A biomimetic Schlemm's canal inner wall: A model to study outflow physiology, glaucoma pathology and high-throughput drug screening. *Biomaterials* **65**, 86–92 (2015).

14. An advanced in vitro model to assess glaucoma onset | ALTEX - Alternatives to animal experimentation. https://www.altex.org/index.php/altex/article/view/1431.

15. Vernazza, S. *et al.* 2D- and 3D-cultures of human trabecular meshwork cells: A preliminary assessment of an in vitro model for glaucoma study. *PLOS ONE* **14**, e0221942 (2019).

16. Waduthanthri, K. D., He, Y., Montemagno, C. & Cetinel, S. An injectable peptide hydrogel for reconstruction of the human trabecular meshwork. *Acta Biomater.* **100**, 244–254 (2019).

17. Li, H. *et al.* A tissue-engineered human trabecular meshwork hydrogel for advanced glaucoma disease modeling. *Exp. Eye Res.* **205**, 108472 (2021).

18. Osmond, M. J., Krebs, M. D. & Pantcheva, M. B. Human trabecular meshwork cell behavior is influenced by collagen scaffold pore architecture and glycosaminoglycan composition. *Biotechnol. Bioeng.* **117**, 3150–3159 (2020).

19. Osmond, M., Bernier, S. M., Pantcheva, M. B. & Krebs, M. D. Collagen and collagen-chondroitin sulfate scaffolds with uniaxially aligned pores for the biomimetic, three dimensional culture of trabecular meshwork cells. *Biotechnol. Bioeng.* **114**, 915–923 (2017).

20. Erickson, C. B. *et al.* In vivo degradation rate of alginate–chitosan hydrogels influences tissue repair following physeal injury. *J. Biomed. Mater. Res. B Appl. Biomater.* **108**, 2484–2494 (2020).

21. Feasibility of Polysaccharide Hybrid Materials for Scaffolds in Cartilage Tissue Engineering: Evaluation of Chondrocyte Adhesion to Polyion Complex Fibers Prepared from Alginate and Chitosan | Biomacromolecules. https://pubs.acs.org/doi/abs/10.1021/bm0400067?casa_token=JFAW1x6sk7cAAAAA%3Abhfoo8m7GTOzfaYg2bIrBI8tKQF4k8T7T-9nMEbtw3wFNNWbjD5gvFtVpWF0QdxlltTSjfT7N3e1SAXv&.

22. Bayr, H. Reactive oxygen species. *Crit. Care Med.* **33**, S498 (2005).

23. Auten, R. L. & Davis, J. M. Oxygen Toxicity and Reactive Oxygen Species: The Devil Is in the Details. *Pediatr. Res.* **66**, 121–127 (2009).

24. Eun, H. S. *et al.* Gene expression of NOX family members and their clinical significance in hepatocellular carcinoma. *Sci. Rep.* **7**, (2017).

25. Liu, R.-M. & Desai, L. P. Reciprocal regulation of TGF-β and reactive oxygen species: A perverse cycle for fibrosis. *Redox Biol.* **6**, 565–577 (2015).

26. Min, S. H., Lee, T.-I., Chung, Y. S. & Kim, H. K. Transforming Growth Factor-β Levels in Human Aqueous Humor of Glaucomatous, Diabetic and Uveitic Eyes. *Korean J. Ophthalmol. KJO* **20**, 162–165 (2006).

27. Pinazo-Durán, M. D. *et al.* Strategies to Reduce Oxidative Stress in Glaucoma Patients. *Curr. Neuropharmacol.* **16**, 903–918 (2018).

28. Ko, M.-L., Peng, P.-H., Hsu, S.-Y. & Chen, C.-F. Dietary deficiency of vitamin E aggravates retinal ganglion cell death in experimental glaucoma of rats. *Curr. Eye Res.* **35**, 842–849 (2010).

29. Das, N. P. Effects of vitamin A and its analogs on nonenzymatic lipid peroxidation in rat brain mitochondria. *J. Neurochem.* **52**, 585–588 (1989).

30. Garcia-Medina, J. J. *et al.* Glaucoma and Antioxidants: Review and Update. *Antioxid. Basel Switz.* **9**, (2020).

31. Bhattacharyya, J., Padmanabha Udupa, E. G., Wang, J. & Sharma, K. K. Mini-alphaB-crystallin: a functional element of alphaB-crystallin with chaperone-like activity. *Biochemistry* **45**, 3069–3076 (2006).

32. Nahomi, R. B. *et al.* Chaperone Peptides of α-Crystallin Inhibit Epithelial Cell Apoptosis, Protein Insolubilization, and Opacification in Experimental Cataracts*,. *J. Biol. Chem.* **288**, 13022–13035 (2013).

33. Nahomi, R. B., DiMauro, M. A., Wang, B. & Nagaraj, R. H. Identification of peptides in human Hsp20 and Hsp27 that possess molecular chaperone and anti-apoptotic activities. *Biochem. J.* **465**, 115–125 (2015).

34. Stankowska, D. L. *et al.* Systemically administered peptain-1 inhibits retinal ganglion cell death in animal models: implications for neuroprotection in glaucoma. *Cell Death Discov.* **5**, 1–15 (2019).

35. Das, S. *et al.* Cerium oxide nanoparticles: applications and prospects in nanomedicine. *Nanomed.* **8**, 1483–1508 (2013).

36. M. Dowding, J., Dosani, T., Kumar, A., Seal, S. & T. Self, W. Cerium oxide nanoparticles scavenge nitric oxide radical (˙NO). *Chem. Commun.* **48**, 4896–4898 (2012).

37. Salehi, B. *et al.* Resveratrol: A Double-Edged Sword in Health Benefits. *Biomedicines* **6**, (2018).

38. Luna, C. *et al.* Resveratrol prevents the expression of glaucoma markers induced by chronic oxidative stress in trabecular meshwork cells. *Food Chem. Toxicol. Int. J. Publ. Br. Ind. Biol. Res. Assoc.* **47**, 198–204 (2009).

39. McKee, C. T. *et al.* The effect of biophysical attributes of the ocular trabecular meshwork associated with glaucoma on the cell response to therapeutic agents. *Biomaterials* **32**, 2417–2423 (2011).

40. Baysal, K., Aroguz, A. Z., Adiguzel, Z. & Baysal, B. M. Chitosan/alginate crosslinked hydrogels: Preparation, characterization and application for cell growth purposes. *Int. J. Biol. Macromol.* **59**, 342–348 (2013).

41. Keller, K. E. *et al.* Consensus recommendations for trabecular meshwork cell isolation, characterization and culture. *Exp. Eye Res.* **171**, 164–173 (2018).

42. Human Myoglobin FASTA Sequence. *Uniprot* https://www.uniprot.org/uniprot/P02144.fasta.

43. Human TGFBeta2 FASTA Sequence. *Uniprot* https://www.uniprot.org/uniprot/P61812.fasta.

44. Bovine Albumin FASTA Sequence. https://www.uniprot.org/uniprot/A0A140T897.fasta.

45. TRI Reagent® Protocol. *Sigma-Aldrich* https://www.sigmaaldrich.com/technical-documents/protocols/biology/tri-reagent.html.

46. Cell Counting Kit-8. *Dojindo Molecular Technologies, Inc.* https://www.dojindo.com/product/cell-counting-kit-8/.

47. Rao, V. R. & Stubbs, E. B. TGF-β2 Promotes Oxidative Stress in Human Trabecular Meshwork Cells by Selectively Enhancing NADPH Oxidase 4 Expression. *Invest. Ophthalmol. Vis. Sci.* **62**, 4–4 (2021).

48. Shah, M. H. *et al.* Nox4 Facilitates TGFβ1-Induced Fibrotic Response in Human Tenon's Fibroblasts and Promotes Wound Collagen Accumulation in Murine Model of Glaucoma Filtration Surgery. *Antioxid. Basel Switz.* **9**, (2020).

49. Susanna, R., De Moraes, C. G., Cioffi, G. A. & Ritch, R. Why Do People (Still) Go Blind from Glaucoma? *Transl. Vis. Sci. Technol.* **4**, (2015).

50. Last, J. A. *et al.* Elastic Modulus Determination of Normal and Glaucomatous Human Trabecular Meshwork. *Invest. Ophthalmol. Vis. Sci.* **52**, 2147–2152 (2011).

51. Campo, G. M., Avenoso, A., Campo, S., Ferlazzo, A. M. & Calatroni, A. Chondroitin sulphate: antioxidant properties and beneficial effects. *Mini Rev. Med. Chem.* **6**, 1311–1320 (2006).

52. Pierce™ BCA Protein Assay Kit. https://www.thermofisher.com/order/catalog/product/23225#/23225.

53. H2DCFDA (H2-DCF, DCF). https://www.thermofisher.com/order/catalog/product/D399.